

# Investigation of the collective properties of excitons in polar semiconductors (ZnO)

V. G. Litovchenko, D. V. Korbutyak, and Yu. V. Kryuchenko

*Institute of Semiconductors, Academy of Sciences of the Ukrainian SSR, Kiev*

Submitted 11 August 1981)

Zh. Eksp. Teor. Fiz. **81**, 1965–1976 (December 1981)

Systematic investigations were made of the exciton–plasma collective effects in a semiconductor with polar binding. Two types of a bulk electron–hole liquid formed at high excitation intensities and relatively high temperatures (above that of liquid nitrogen). A quasi-two-dimensional liquid was observed on the surface of ZnO subjected to a low-dose argon ion treatment. The properties of a layer liquid, distinguishing it from the bulk form, were investigated. An analysis was made of the phase diagrams for bound bulk and surface liquids.

PACS numbers: 71.35. + z

## 1. INTRODUCTION

The possibility of formation of an electron–hole (EH) liquid in direct-gap semiconductors has long been regarded as doubtful, although the existence of the liquid has been proved for Ge and Si (Refs. 1–3). However, as first demonstrated by Keldysh and Silin,<sup>4</sup> the electron–phonon interaction stabilizes such a liquid even in simple (single-valley) direct-gap structures. This problem has been investigated both theoretically<sup>5</sup> and experimentally.<sup>6–10</sup> In particular, it has been found<sup>9,10</sup> that in the case of a quasitwo-dimensional EH liquid formed at the GaAs–Si<sub>3</sub>N<sub>4</sub> interface an increase in its binding energy estimated on the basis of Ref. 4 (allowing for the change in the effective electron mass  $m_e$  and in the permittivity  $\epsilon$  on the semiconductor surface) is very considerable.

We investigated the collective properties of excitons in a wide-gap semiconductor ZnO. This material is characterized by a high proportion of the polar binding and also has high values of the exciton binding energy  $E_{ex} = 59$  meV (Ref. 11) and of the electron–phonon coupling constant, so that we can expect a high critical temperature  $T_c$  of the existence of any EH liquid ( $kT_c \approx 0.1E_{ex}$ —Ref. 1). Finally, it is known that the surface localization effects (presence of dark or light-induced inversion and quantum channels, etc.) are manifested very strongly by ZnO. All these properties have made it desirable to investigate in detail various exciton and plasma collective effects in the polar semiconductor ZnO.

We investigated the photoluminescence spectra of ZnO single crystals of sufficiently high quality at various optical excitation rates ( $L_{max} \approx 4$  MW/cm<sup>2</sup>) in the temperature range 4.2–120 °K. This photoluminescence was excited by pulses from an LGI-21 nitrogen laser of the  $\lambda = 3371$  Å wavelength. The laser beam was focused sharply on a sample. This beam was attenuated, as necessary, by glass filters. The luminescence was analyzed with an SDL-1 monochromator (linear dispersion 8 Å/mm) using the photoelectric method to record the spectra.

We used ZnO samples with natural surfaces and those treated by low-energy ion bombardment ( $Ar^+$ ,  $E = 1$

keV,  $D \approx 10^{15}$  cm<sup>-2</sup>). In the latter case a semimetallic thin layer capable of localizing electrons on the surface could form.<sup>12</sup>

When the excitation was weak, the edge luminescence of ZnO was dominated by bands due to radiative recombination of excitons bound to shallow impurities. An increase in the excitation power density  $L$  on the long-wavelength side of the luminescence line due to excitons bounded to shallow donors revealed new lines which transformed into a wide photo-luminescence band on further increase in  $L$ . A detailed analysis of the intensities, profiles, and energy positions of these bands was carried out for various values of  $L$  and it made it possible to identify their polyexciton origin.<sup>13</sup>

At high excitation rates ( $L \approx 4$  MW/cm<sup>2</sup>) there were two types of bound EH liquid characterized by fairly high (above the liquid nitrogen temperature  $T_{N_2}$ ) critical temperatures. The phase diagram was plotted for one of the types of bound EH liquid. Low-dose argon ion bombardment localized this liquid on the surface, which made it possible to study the properties of such a localized liquid in comparison with the bulk form of the liquid.

## 2. BOUND ELECTRON-HOLE LIQUID

Figures 1 and 2 show the results of an investigation of the profiles and half-widths of the bands of the original and ion-bombarded ZnO crystals obtained at different optical excitation rates ( $L_{max} \approx 4$  MW/cm<sup>2</sup>,  $T = 4.2$  °K). An increase in the rate of excitation transformed narrow lines of  $m$  exciton–impurity complexes described earlier<sup>13</sup> into a wide band  $Q_1$ .

The origin of the wide photoluminescence bands exhibited by ZnO in the 3.34–3.36 eV photon energy range at low temperatures and high rates of excitation is still a matter of controversy. These bands have been attributed to the radiative decay of biexcitons,<sup>14</sup> to the interaction of bound excitons with electrons,<sup>15</sup> and to the formation of a free EH liquid.<sup>16</sup>

The band  $Q_1$  had the characteristic features of a bound EH liquid: 1) it was located on the long-wavelength side of the bound-exciton luminescence line  $J_1$ ;

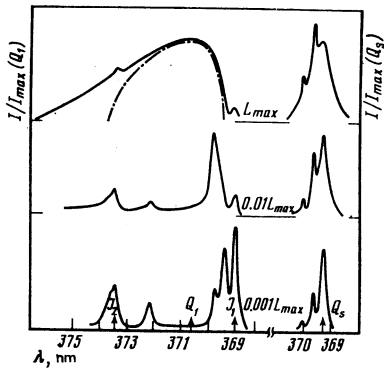


FIG. 1. Photoluminescence spectra of the original (on the left) and ion-bombarded (on the right) ZnO recorded at different rates of excitation. The chain curve shows the theoretically calculated profile of a line due to an electron-hole liquid corresponding to  $n_0 \approx 5 \times 10^{18} \text{ cm}^{-3}$ .

2) an increase in  $L$  broadened considerably the long-wavelength wing of the luminescence line but hardly affected the energy position of its short-wavelength wing; 3) the half-width  $H$  of the  $Q_1$  line increased greatly when the excitation rate became  $L \approx 0.4L_{\max}$  but remained constant at higher values of  $L$  (Fig. 2); 4) an increase in the rate of excitation resulted in a super-linear rise of the intensity  $I \propto L^n$ , where  $n = 1.7-2$ ; 5) variation of the temperature of the sample  $T$  in the range 4–40 °K did not alter greatly the half-width, in agreement with the corresponding behavior of the carrier density in a degenerate exciton liquid:  $H \propto n^{2/3} \propto (1 - \delta_n T^2)^{2/3}$ , where  $\delta_n$  is an entropy parameter (Figs. 3a and 3b). Only beginning from  $T \geq 40-50$  °K was there a gradual shift of the maximum of this band toward longer wavelengths. At the same time a new wide peak  $Q_2$  ( $H \approx 35$  meV) appeared in the long-wavelength wing and the half-width of this peak decreased on increase in temperature. This indicated a redistribution of nonequilibrium EH pairs from one type of liquid (corresponding to the  $Q_1$  line) localized at the binding centers of the  $J_1$  excitons to another ( $Q_2$ ) localized at deeper  $J_2$  centers,<sup>11</sup> and consequently at these temperatures the EH liquid with a lower binding energy became unstable and started to evaporate gradually. This corresponded to enhancement of the recombination processes in the exciton liquid (due to, for example, temperature dependences of the Auger process coefficients<sup>18</sup>).

The agreement between the theoretical and experimental dependences  $H(T)$  gave the following values of the entropy parameter:  $\delta_n \approx (1-3) \times 10^{-4} \text{ K}^{-2}$  and  $\delta_n$

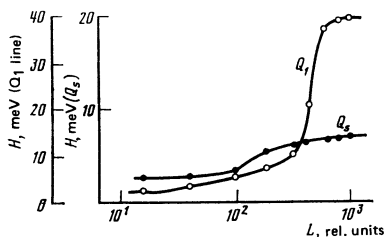


FIG. 2. Dependences of the half-widths  $H$  of the  $Q_1$  and  $Q_2$  bands on  $L$ .

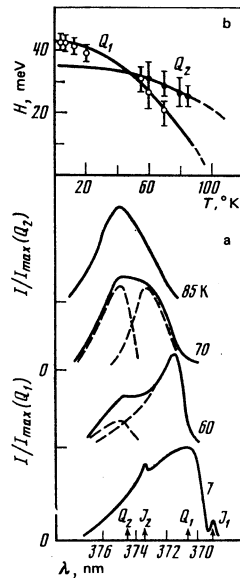


FIG. 3. a) Photoluminescence spectra of the original ZnO at various temperatures obtained for  $L \approx 4 \text{ MW/cm}^2$ . The dashed curves identify the  $Q_1$  and  $Q_2$  bands. b) Temperature dependences of the half-width  $H$  of the electron-hole liquid lines  $Q_1$  and  $Q_2$ : the points are the experimental results and the continuous curves are calculated theoretically from  $H \approx H_0(1 - \delta_n T^2)^{2/3}$ .

$\approx 7 \times 10^{-5} \text{ K}^{-2}$  for the  $Q_1$  and  $Q_2$  bands, respectively. The lower value of  $\delta_n(Q_2)$  indicated a higher stability and, consequently, a higher critical temperature  $T_c$  of an EH liquid. For example, in the case of Ge we have  $\delta_n \approx 1 \cdot 10^{-2} \text{ K}^{-2}$  and  $T_c \approx 6.5$  °K (Ref. 19), whereas for Si we find that  $\delta_n \approx 7 \cdot 10^{-4} \text{ K}^{-2}$  and  $T_c \approx 33$  °K (Ref. 20) and at the GaAs-Si<sub>3</sub>N<sub>4</sub> interface we obtain  $\delta_n \approx 1.1 \cdot 10^{-2} \text{ K}^{-2}$ , and  $T_c \approx 8.5$  °K (Ref. 10).

It should be noted that the long-wavelength wing of the experimental photoluminescence band profile  $Q_1$  (Fig. 1) was described satisfactorily by the well-known formula for the recombination radiation emitted by EH pairs in direct-gap semiconductors (see, for example, Ref. 21):

$$I_{\text{PL}}(E) \sim \sum_{h_n = -h_h = h} f_{e,h} \delta(E - \mathcal{E}_e(k) - \mathcal{E}_h(k)), \quad (1)$$

where  $f_{e,h}$  are the distribution functions of electrons and holes,  $\mathcal{E}_{e,h}(k)$  are the dispersion laws of electrons and holes, and  $E$  is the energy measured from the long-wavelength edge of the photoluminescence band. This is additional evidence in support of the liquid-plasma state in crystals with a strong influence of the polar type of binding, which has been suggested also in several theoretical investigations.<sup>4,5</sup> However, some features of the behavior of excitons and of any EH liquid in such crystals are still not clear.<sup>22</sup> This applies, in particular, to the high binding energy of excitons in polar crystals and to the considerable discrepancy between the theory and experiment in respect of the long-wavelength wing of the EH liquid band (Fig. 1). This has been established for a number of direct-gap semiconductors with a considerable contribution of the ionic type of binding, such as CdS (Ref. 21) and GaAs (Refs. 8 and 10), for which the degree of ionicity  $\Delta E_{\text{ion}}$  is 15 and 4%, respectively.<sup>23</sup> In the case of ZnO, the value

of  $\Delta E_{\text{ion}}$  is even greater and it amounts to 60% (Ref. 23). In our opinion, this discrepancy may be due to a considerable influence of the plasmon-phonon interaction. In fact, strong exciton-phonon and plasmon-phonon interactions have been reported for ZnO in several investigations (see, for example, Ref. 17). In our case the phonon energies are 1–10 meV, which corresponds to the participation of local phonons or the generation of hyperphonons, which is important at the laser excitation rates employed. Another mechanism may be a plasmon-recombination dissipation of energy. The energy of the main plasma oscillation mode (3–10 meV according to Ref. 24) also agrees with the observed additional line broadening.

An estimate of the radius of an EH drop (for the  $Q_1$  line) gives a relatively small value of  $R \approx 3\nu_T \tau N / 4n_0 \sim 10^{-6}$  cm. This value is obtained assuming that the effective exciton lifetime is  $\tau \approx 10^{-9}$  sec (Ref. 16). Hence, it follows that the total concentration of the condensation centers is  $N_t \approx 10^{12}$  cm $^{-3}$ . A similar value is also obtained from the more accurate relationship<sup>25</sup>

$$R_{\text{min}} \approx \left( 6\gamma \frac{\sigma \nu_T \tau_0 n_T}{n_0 k T n_0} \right)^{1/2}$$

when the surface tension is assumed to be  $\sigma \approx 10^{-2} - 10^{-3}$  erg/cm $^2$ , which is typical of a liquid with a high carrier density.<sup>26</sup>

### 3. OBSERVATION OF A SURFACE ELECTRON-HOLE LIQUID

Ion bombardment makes it possible to control the localization characteristics of the liquid described above, creating conditions favorable to its formation on the surface.<sup>27</sup> This type of treatment alters the stoichiometric composition by increasing the excess of Zn atoms and this, as is known, creates semimetallic islands as well as simple ("shallow") surface defects. In view of the giant oscillator strengths associated with exciton complexes,<sup>28</sup> such defects act as exciton capture centers and when the excitation intensity is increased further, an EH liquid is formed. Consequently, at high concentrations of these centers we can expect a basically different (not dependent on the formation of large many-particle exciton-impurity complexes) way of formation of a liquid-plasma EH liquid. In fact, an increase in the rate of excitation (and a corresponding enhancement in the rate of binding of excitons to an increasing number of centers) results in the overlap of the wave functions of neighboring exciton-impurity complexes, which is completed by the formation of a continuous quasitwo-dimensional layer of an EH liquid. The interest in this way of formation of an EH liquid is due to the fact that it makes it possible to study these special properties of a quasitwo-dimensional liquid since the condensation centers are then located in a very thin layer  $\Delta x \approx r_{\text{ex}}$  ( $r_{\text{ex}}$  is the exciton radius).

Our results are plotted in Fig. 1. A new line  $Q_3$  was emitted by the bombarded surface of ZnO: it had a profile and energy position different from the bulk band  $Q_1$ . The quasitwo-dimensional nature of the observed EH

liquid was manifested by its characteristic properties: 1) a smaller power exponent,  $n_3 \approx 1.2$ , in the  $I(L)$  dependence; 2) a shift toward higher values (by  $\approx 10\%$ ) of the binding energies of the exciton-impurity complexes and of the EH liquid; 3) line narrowing compared with the bulk (reduction in the half-width  $H$  from 42 to 8 meV).

The reduction in the power exponent of the dependence of the luminescence intensity on the excitation rate is, in fact, due to a change in the shape of the drops and it is essentially due to the directional growth of the latter. In the case of pancake-shaped drops the power exponent should be close to  $n \approx 2$  (as found experimentally in Ref. 9), whereas in the case of planar drops it should be close to  $n \approx 1$ , as found in our study.

An increase in the binding energy of the EH liquid (and of free excitons) is due to a number of factors, some of which can be described within the framework of the macroscopic approximation (reduction in the symmetry of the system),<sup>29</sup> whereas others require allowance for the surface microstructure (changes in the lattice and in the energy band structure, influence of the phases in contact). In a purely two-dimensional case we can expect a severalfold increase in the binding energy  $\varphi$  of an EH liquid.<sup>29,30</sup> The rise of  $\varphi$  is not as large in our case and this is clearly due to a number of reasons, primarily because at the energies of ion-plasma treatments used in our experiments the thickness of the layer of localization of the condensation centers  $\Delta x$  is comparable with the exciton radius. Additionally, the attractive Coulomb interaction of excitons is partly screened by the metallized islands on the surface. Moreover, the energy band structure of a crystal may be modified greatly by intense ion bombardment and this structure determines the parameters of both excitons and of an EH liquid. Finally, we cannot exclude the possibility that in the case of sufficiently strongly localized excitons the process of condensation does not produce a metallic state but an insulating one. It follows from Ref. 31 that the condensation to an insulating state occurs at much lower carrier densities and this is typical of an ion-treated surface.

Narrowing of the luminescence line of a quasitwo-dimensional EH liquid is predicted in Ref. 30 on the basis of a calculation of the line profile described by

$$I(\omega) \sim \int G_{\nu c}(\omega) k dk;$$

here,  $G_{\nu c}(\omega)$  is the spectral function of the density of electrons and holes. The physical reason for the narrowing of the  $Q_s$  line compared with  $Q_1$ , observed in our study, is a reduction in the density of carriers in a degenerate EH liquid (it is estimated that the reduction is from  $5 \times 10^{18}$  cm $^{-3}$  to  $\sim 10^{18}$  cm $^{-3}$ ) because of a reduction in the influence of the surface tension forces for a liquid of planar geometry.

The quasitwo-dimensional nature of a degenerate plasma in the case of a continuous surface layer means that in this situation we may expect manifestation of the quantization of an electron gas in the transverse direction. Electrons are then driven to the surface by the potential barrier of local centers and by

the image forces, whereas they move freely along the surface. If the width of the confining potential well  $L_z$  is less than the de Broglie wavelength  $\lambda = 2\pi/k \sim \hbar/(2kTm^*)^{1/2}$ , the spectrum of free electrons becomes discrete<sup>32</sup>:

$$E = \sum_{x,y} \frac{\hbar^2 k_{x,y}^2}{2m_{x,y}^*} + \frac{\hbar^2 \pi^2}{2m_z^*} \frac{(1+n)^2}{L_z^2}. \quad (2)$$

The distance between two-dimensional subbands is governed by the width of the well at the point where the levels are passing. For a rectangular well we have  $L = \text{const}$ , whereas for a Coulomb collective barrier we find that  $L = L(z)$ . In particular, if we adopt the triangular approximation, we find that the distance between the levels is given by

$$\Delta E = \frac{1}{2} \left[ \frac{(3\pi e \hbar E_s)^2}{m_z^*} \right]^{1/2} \left( n + \frac{3}{4} \right). \quad (3)$$

For  $L \approx 10^{-6} - 10^{-7}$  cm we have  $\Delta E \approx 10^{-4} - 10^{-2}$  eV (Ref. 32), which corresponds to the infrared part of the spectrum. It follows that the appearance of a two-dimensional quantum plasma may give rise to a number of effects that are not exhibited by a three-dimensional (nonquantized) plasma. For example, transitions between two dimensional quantum subbands with a density of states  $\kappa = N_{2D}/E_{2D} \sim (2\pi a_B^*)^{-2}/E_{2D} \sim m^*/2\pi\hbar \approx 10^{10} - 10^{12}$  cm<sup>-2</sup> may give rise to various oscillation effects in the photoconductivity, infrared absorption, luminescence in the short-wavelength wing of a band, etc.

#### 4. ANALYSIS OF THE PHASE DIAGRAM OF AN ELECTRON-HOLE LIQUID IN ZnO

It is difficult to construct the gas-liquid phase diagram for a direct-gap semiconductor because the nonequilibrium carrier lifetime ( $\tau \leq 10^{-9}$  sec) is short so that a full equilibrium is not established in the two-phase system under discussion. However, detailed investigations of the temperature dependences of the profile of a luminescence line due to an EH liquid allow us to find quite accurately the quasiequilibrium density in the liquid phase (liquid branch). The gas branch of the phase diagram is deduced from measurements of the threshold density of EH pairs corresponding to the appearance of the EH liquid line.

Figure 4 shows the phase diagram for the EH liquid corresponding to  $Q_1$ , as deduced from an analysis of the experimental results (I) and calculated (II) for an EH liquid in ZnO in accordance with the theory.<sup>4,5,7</sup> The thermodynamic equilibrium density of the exciton gas found by equating the chemical potentials for the gas and the liquid is given by

$$n_T = 4(MkT/2\pi\hbar^2)^{3/2} e^{-\varphi/k_0 T}, \quad (4)$$

where  $M$  is the exciton mass and  $\varphi$  is the binding energy of an EH liquid.

The considerable discrepancy between the theoretical phase diagram and the experimental data for direct-gap semiconductors is due to nonequilibrium of the gas-liquid system.<sup>33</sup> Moreover, at high carrier densities when the plasma frequency  $\omega_p$  becomes compara-

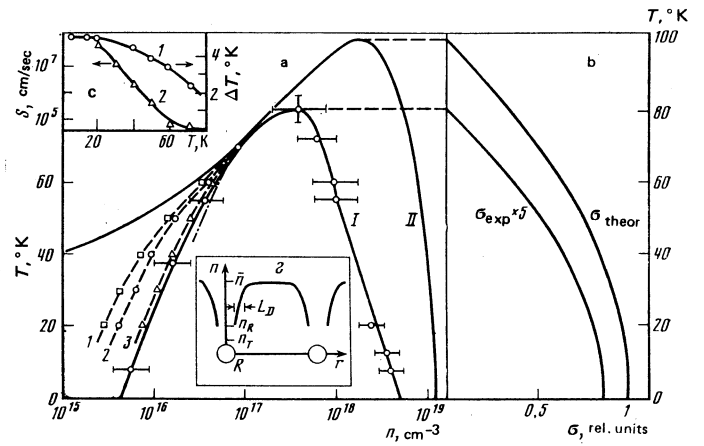


FIG. 4. a) Experimental (of an electron-hole liquid corresponding to  $Q_1$ ) (I) and theoretically calculated (II) gas-liquid phase diagrams for ZnO. Curves 1, 2, and 3 are the dependences  $n_R(T)$  for  $R = 10^{-5}$ ,  $10^{-6}$ , and  $10^{-7}$  cm and  $S = 0$ . The chain curve is the Mott transition line. b) Temperature dependences of the surface tension  $\sigma$  for an electron-hole liquid in ZnO. c) Curve 1 represents the overheating  $\Delta T$  of an electron-hole liquid corresponding to  $Q_1$  found by matching the theoretical and experimental luminescence band profiles; curve 2 gives the critical value of the parameter  $S$  corresponding to  $n_R = n_T$ . d) Schematic representation of the distribution of the exciton (electron-hole gas) density near the condensation centers.

ble with the frequency of longitudinal optical phonons  $\omega_{LO}$ , we may expect oscillations of the mixed plasmon-phonon type which influence the condensation energy of an EH liquid.

Allowance for the interaction of carriers with LO phonons gives corrections to the exchange and correlation energies, which increases the condensation energy  $\varphi$  and stabilizes a metallic EH liquid in direct-gap semiconductors.<sup>4,5,34</sup> Moreover, the condensation energy of such a liquid depends also on the relationship between  $E_{ex}$  and  $\hbar\omega_{LO}$  (Ref. 35). Therefore, the condensation energy of a liquid and, consequently,  $T_c$ ,  $n_0$ , and  $n_c$  depend in a complex manner on a number of parameters:  $E_{ex}$ ,  $\omega_p$ ,  $\omega_{LO}$ ,  $\epsilon_0$ ,  $\epsilon_\infty$ , etc. (Table I).

Figure 5 shows the dependences of  $T_c$ ,  $n_c$ , and  $n_0$  on  $E_{ex}$  for various direct-gap semiconductors. These dependences are linear only at low values of  $E_{ex}$  in accordance with Ref. 1 and they become sublinear in the range  $E_{ex} \geq 20 - 30$  meV. Semiconductors with a large exciton binding energy  $E_{ex}$  are characterized also by a strong ionicity (Table I).

We shall now consider the special features of the phase diagram (Fig. 4). First of all, we note that the critical temperature ( $T_c \approx 100$  K) is in our case close to that calculated for a free EH liquid allowing for the LO mechanism<sup>7</sup>:  $T_c \approx 107$  K. The main difference between the theoretical and experimental phase diagrams is that the experimental diagram is narrower and has a lower value of  $T_c$  ( $T_c^{exp} \approx 80$  K). Moreover, the experimental gas branch of the phase diagram is shifted relative to the thermodynamic equilibrium line in the direction of higher densities, particularly at low tempera-

TABLE I.

| Semiconductor | $E_{ex}$ , meV | $\hbar\omega_{LO}$ , meV | $\epsilon_0$ | $\epsilon_{\infty}$ | $E_{ion}$ , % | Theory                    |                           |            |              | Ref.        |
|---------------|----------------|--------------------------|--------------|---------------------|---------------|---------------------------|---------------------------|------------|--------------|-------------|
|               |                |                          |              |                     |               | $10^{-17}n_0$ , $cm^{-3}$ | $10^{-17}n_c$ , $cm^{-3}$ | $T_c$ , °K | $\phi$ , meV |             |
| GaAs          | 3.5            | 36.2                     | 12           | 10.1                | 4             | 0.34                      | 0.043                     | 6.5        | 1.8          | [7]         |
| CdTe          | 11             | 21.3                     | 10.9         | 7.2                 | 4             | 2.9                       | 0.44                      | 18         | 0.9          | [7]         |
| GdSe          | 15             | 26.1                     | 10.6         | 7.0                 | 12            | 8.3                       | 1.2                       | 30         | 5            | [6]         |
| GaP           | 20             | 51.0                     | 10.0         | 8.2                 | 7             | 70                        | —                         | —          | 10           | [5]         |
| CdS           | 27             | 36.8                     | 8.9          | 5.4                 | 15            | 550                       | 7.8                       | 64         | 14           | [6]         |
| ZnS           | 36             | 43.6                     | 8.3          | 5.0                 | 20            | 83                        | 14                        | 79         | 12           | [7]         |
| ZnO           | 59             | 72.0                     | 7.9          | 3.6                 | 60            | 120                       | 20                        | 107        | -9           | [33]        |
|               |                |                          |              |                     |               |                           |                           | 100        | —            | Our results |

| Semiconductor | Experiment                |                           |            |              | Ref.        |
|---------------|---------------------------|---------------------------|------------|--------------|-------------|
|               | $10^{-17}n_0$ , $cm^{-3}$ | $10^{-17}n_c$ , $cm^{-3}$ | $T_c$ , °K | $\phi$ , meV |             |
| GaAs          | 0.3                       | —                         | —          | 4.7          | [7]         |
| CdTe          | —                         | —                         | —          | —            | —           |
| GdSe          | 4                         | —                         | —          | 2            | [6]         |
| GaP           | 60                        | —                         | 40         | 14           | [33]        |
| CdS           | 20                        | 8                         | 55         | 13           | [6]         |
| ZnS           | —                         | —                         | —          | —            | —           |
| ZnO           | 10                        | —                         | 70         | 22           | [16]        |
|               | 50                        | 4                         | 80         | 26           | Our results |

tures. For example, at  $T=10^\circ K$  the degree of supersaturation is  $\ln(n_{exp}/n_T) \approx 10$ , where  $n_{exp}$  is the threshold density (found experimentally) corresponding to the appearance of an EH liquid and  $n_T$  is the thermodynamic-equilibrium value of this density. The high degree of supersaturation is a direct consequence of the nonequilibrium of the EH gas, which is due to its short lifetime compared with the lifetime of the condensed liquid  $\tau_l$ .

A calculation of the gas branch of the nonequilibrium phase diagram was made on the assumption that a distance between the condensation centers is much greater than the diffusion length  $L_D$ , so that  $L_D^3 N_k \ll 1$  ( $N_k$  is the concentration of the condensation centers), so that carriers are attracted to the condensation centers only from a small proportion of the sample (Fig. 4d). Therefore, the experimental average density  $\bar{n}$  in the excited part of the sample is much higher than the local value at a point  $r$  close to a condensation center. The dependence of the exciton density  $n(r)$  on the coordinate

$r$  under steady-state conditions is given by

$$D \operatorname{div} \operatorname{grad} n - n/\tau_0 + g = 0. \quad (5)$$

The boundary condition is of the form

$$D \operatorname{grad} n|_{r=R} = \gamma[n(R) - n_T]v_r + S n(R). \quad (6)$$

We have allowed here for the possibility of additional recombination at a condensation center characterized by a velocity  $S$ ;  $\gamma$  is the carrier capture coefficient;  $R$  is the drop radius;  $r$  is the running coordinate.

A solution of Eq. (5) is of the form

$$n(r) = \bar{n} - \frac{\gamma[n(R) - n_T]v_r + S n(R)}{D(1 + R/L_D)} \frac{R^2}{r} e^{-(r-R)/L_D}. \quad (7)$$

Near the surface if a drop ( $r \approx R$ ) the density  $n_R$  is related to  $\bar{n}$  by

$$n_R(T) = \bar{n} \Phi(R, S, T), \quad (8)$$

where  $\Phi(R, S, T) < 1$  and this factor is described by

$$\Phi(R, S, T) = \left[ 1 + \frac{\gamma R v_r}{D(1 + R/L_D)} \frac{n_T}{\bar{n}} \right] / \left[ 1 + \frac{R(\gamma v_r + S)}{D(1 + R/L_D)} \right]. \quad (9)$$

The values of  $n_R(T)$  were calculated for different parameters  $R$  and  $S$ , including those estimated from the experimental results. As expected, they lie in the interval between those calculated theoretically for the equilibrium case  $n_T$  and the experimentally determined average values  $\bar{n}$  (Fig. 4a). Under normal conditions we have  $R/L_D \ll 1$  and the relationship describing  $\Phi$  simplifies to

$$\Phi(R, S, T) \approx \left[ 1 + \frac{\gamma R v_r n_T}{D \bar{n}} \right] / \left[ 1 + \frac{R(\gamma v_r + S)}{D} \right]. \quad (10)$$

If  $\gamma \approx 1$  and  $n_T/\bar{n} \ll 1$ , we have

$$\frac{n_R}{\bar{n}} \approx \frac{v_R}{v_r + S}, \quad (11)$$

where  $v_R = D/R$ .

It therefore follows that if  $S < v_T$ , the ratio  $n_R/\bar{n} = D/v_T R$  is determined directly by the drop radius. Under these conditions the density near a drop is governed by a local sink or (if  $S > v_T$ ) by the recombination process, and the arrival of carriers by diffusion is not the limiting factor. At very high values of this parameter  $S = S_{cr}$  we can have such a relationship  $n_R \leq n_T$  for which the condensation does not occur at all. The dependences of the values of  $S_{cr}$  found from Eqs. (8) and (9) and the condition  $n_R = n_T$  are plotted in Fig. 4c.

The second reason for the discrepancy between the experimental gas branch and that found theoretically is the nonideal nature of the EH gas.<sup>36</sup> In this case an increase in  $\tau$  reduces the influence of nonequilibrium. Moreover, the experimental points are close to the Mott transition line calculated from  $L_{scr}/a_{ex} \approx 1.19$  and this demonstrates that the gas part of the phase diagram is distorted only slightly near the maximum (Fig. 4).

In the case of the liquid branch the experimental data correspond to lower carrier densities in an EH liquid than that predicted by the theoretical equilibrium curve. Evaporation from an EH liquid becomes easier when

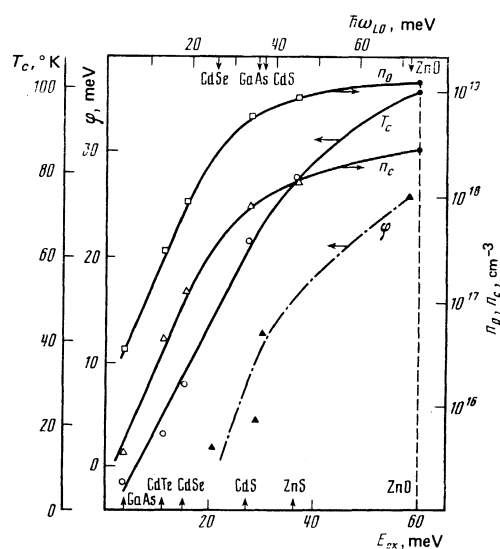


FIG. 5. Dependences of  $n_0$ ,  $n_c$ , and  $T_c$  on the exciton binding energy  $E_{ex}$  for various semiconductors and the dependences of the condensation energy  $\phi$  on  $\hbar\omega_{LO}$ .

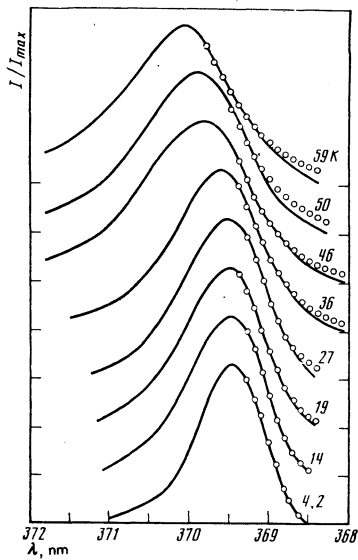


FIG. 6. Experimental (continuous curves) and theoretical (points) profiles of the short-wavelength wing of the  $Q_s$  band at various temperatures.

$\alpha_l = n_l^{\text{exp}}/n_l^{\text{theor}} \approx 5$  and it is mainly due to the lower stability of the EH liquid state under nonequilibrium conditions. Consequently, under these conditions there is a considerable reduction in the surface tension  $\sigma$  described by<sup>26</sup>

$$\sigma(T) = \sigma(0) [1 - (T/T_c)^2]. \quad (12)$$

The temperature dependences of  $\sigma_{\text{theor}}$  and  $\sigma_{\text{exp}}$  are plotted in Fig. 4b.

We can thus see that in spite of nonequilibrium of the EH gas (which is typical of direct-gap semiconductors), a strong influence of the polar interaction ensures a considerable increase in the stability of the various collective effects and makes it possible to observe these effects at fairly high temperatures and at relatively low excitation rates.

The phase diagram of a two-dimensional EH liquid was plotted by analogy of the diagram described above for a three-dimensional liquid. The profile of the short-wavelength wing of the  $Q_s$  band was matched at various temperatures employing a formula describing radiative recombination in a two-dimensional EH liquid (Fig. 6):

$$I'(\hbar\omega) = \left\{ 1 + \exp \left[ \frac{1}{k_0 T} \left( \frac{m_h}{m_e + m_h} E - \mu_e^T \right) \right] \right\}^{-1} \times \left\{ 1 + \exp \left[ \frac{1}{k_0 T} \left( \frac{m_e}{m_e + m_h} E - \mu_h^T \right) \right] \right\}^{-1}, \quad (13)$$

where

$$\mu_{e,h}^T/k_0 T = \ln(\exp(\mu_{e,h}^0/k_0 T) - 1), \quad \mu_{e,h}^0 = \pi \hbar^2 n/m_{e,h}.$$

The phase diagram of a two-dimensional EH liquid formed on an ion-bombarded ZnO surface is plotted in Fig. 7. The temperature dependence of the density of the liquid phase is found from the photoluminescence line profile described in terms of the three-dimensional model [Eq. (1)] but with a strongly anisotropic effective electron mass; this results in a strong bending of the

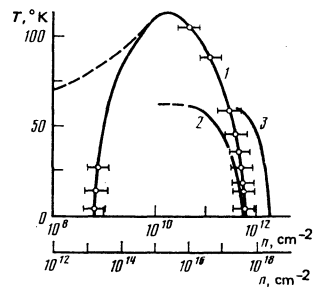


FIG. 7. Phase diagram of an electron-hole liquid corresponding to  $Q_s$  calculated for the two-dimensional model (curve 1). The dashed curve is the equilibrium gas branch of the phase diagram for  $\varphi = 72$  meV; curves 2 and 3 are the temperature dependences of the density in the liquid phase calculated from the three-dimensional model but for different degrees of the anisotropy of the electron mass (2 -  $m_{e\parallel} = m_{e\perp} = 0.3m_0$ ; 3 -  $m_{e\parallel} = 30m_0$ ,  $m_{e\perp} = 0.3m_0$ ).

liquid branch in the direction of lower densities (Fig. 7) on increase in temperature, which is in conflict with the experimental data. In fact, the critical temperature of the existence of the two-dimensional EH liquid observed in our experiments is  $T_c \approx 100$  °K; however, if the profile of the  $Q_s$  band is described by means of the three-dimensional model, the value of  $T_c$  should be considerably higher. This is due to the quasitwo-dimensional nature of the EH liquid on the ion-bombarded surface of ZnO, which is discussed above.

The theoretical gas branch of the phase diagram passes through a region corresponding to the critical state of an EH liquid ( $n_c, T_c$ ), i. e., it completes the phase diagram on the gas side if the condensation energy is assumed to be not  $\varphi \approx E_{\text{ex}} - E_i \approx 17$  meV but  $\varphi = \hbar\omega_{LO} = 72$  meV. Clearly, this value of  $\varphi$  is due to the fact that in our case the condensation occurs at bound excitons and it is known that the transition of excitons from a free to a bound state occurs mainly as a result of scattering by longitudinal optical phonons.

The authors are grateful to L. V. Keldysh, V. L. Bonch-Bruевич, and V. V. Vladimirov for discussing some of the results.

<sup>1</sup>In this range of energies we can expect the lines due to the phonon replicas of free excitons.<sup>17</sup> However, the half-width and the intensities of these replicas are much lower than those of the band  $Q_2$  observed by us.

<sup>2</sup>It should be noted that the factor preventing the condensation of an EH liquid on the surface, namely the repulsive influence of the phonon wind,<sup>27</sup> is not important because of the nonspecularity of the investigated surface and also because of the effective attraction by surface mechanical fields and favorable conditions from the point of view of the exciton and condensate binding energies.

<sup>3</sup>L. V. Keldysh, Proc. Ninth Intern. Conf. on Physics of Semi-conductors, Moscow, 1968, Vol. 2 publ. by Nauka, Leningrad (1968), p. 1303; Sb. Éksitony v poluprovodnikakh (pod red. B. M. Vula) [in: Excitons in Semiconductors (ed. by B. M. Vul)], Nauka, M., 1971, p. 5.

<sup>4</sup>Ya. E. Pokrovskii and K. I. Svistunova, Pis'ma Zh. Eksp. Teor. Fiz. 9, 435 (1969) [JETP Lett. 9, 261 (1966)].

<sup>5</sup>V. S. Bagaev, T. I. Galkina, O. V. Gogolin, and L. V. Kel-

- dysch, Pis'ma Zh. Eksp. Teor. Fiz. 10, 309 (1969) [JETP Lett. 10, 195 (1969)].
- <sup>4</sup>L. V. Keldysh and A. P. Silin, Zh. Eksp. Teor. Fiz. 69, 1053 (1975) [Sov. Phys. JETP 42, 535 (1975)].
- <sup>5</sup>G. Beni and T. M. Rice, Phys. Rev. Lett. 37, 874 (1976); Solid State Commun. 23, 871 (1977).
- <sup>6</sup>R. F. Leheny and J. Shah, Phys. Rev. Lett. 38, 511 (1977); 37, 871 (1976).
- <sup>7</sup>M. Rosler and R. Zimmermann, Phys. Status Solidi B 83, 85 (1977).
- <sup>8</sup>B. V. Stopachinskiĭ, Zh. Eksp. Teor. Fiz. 72, 592 (1977) [Sov. Phys. JETP 45, 310 (1977)].
- <sup>9</sup>V. Z. Zuev, D. K. Korbutyak, V. G. Litovchenko, L. F. Gudymenko, and E. M. Gule, Zh. Eksp. Teor. Fiz. 69, 1289 (1975) [Sov. Phys. JETP 42, 659 (1975)].
- <sup>10</sup>V. A. Zuev, D. V. Korbutyak, Yu. V. Kryuchenko, and V. G. Litovchenko, Fiz. Tverd. Tela (Leningrad) 20, 2908 (1978) [Sov. Phys. Solid State 20, 1680 (1978)].
- <sup>11</sup>D. G. Thomas, J. Phys. Chem. Solids 15, 86 (1960).
- <sup>12</sup>V. A. Zuev, D. V. Korbutyak, M. V. Kurik, V. G. Litovchenko, A. Kh. Rozhko, and P. A. Skubenko, Pis'ma Zh. Eksp. Teor. Fiz. 26, 455 (1977) [JETP Lett. 26, 327 (1977)].
- <sup>13</sup>V. G. Litovchenko, V. N. Babentsov, D. V. Korbutyak, and M. T. Ivaniĭchuk, Pis'ma Zh. Eksp. Teor. Fiz. 30, 578 (1979) [JETP Lett. 30, 544 (1979)].
- <sup>14</sup>J. M. Hvam, Phys. Status Solidi B 63, 511 (1974); Solid State Commun. 27, 1347 (1978).
- <sup>15</sup>C. Klingshirn, Phys. Status Solidi B 71, 547 (1975).
- <sup>16</sup>T. Skettrup, Solid State Commun. 23, 741 (1977).
- <sup>17</sup>R. L. Weiher and W. C. Tait, Phys. Rev. 166, 791 (1968).
- <sup>18</sup>V. A. Zuev, V. G. Litovchenko, and G. A. Sukach, Fiz. Tekh. Poluprovodn. 9, 1641 (1975) [Sov. Phys. Semicond. 9, 1083 (1975)].
- <sup>19</sup>G. A. Thomas, T. M. Rice, and J. C. Hensel, Phys. Rev. Lett. 33, 219 (1974).
- <sup>20</sup>A. F. Dite, V. G. Lysenko, and V. B. Timofeev, Phys. Status Solidi B 66, 53 (1974).
- <sup>21</sup>V. G. Lysenko, V. I. Revenko, T. G. Tratas, and V. B. Timofeev, Zh. Eksp. Teor. Fiz. 68, 335 (1975) [Sov. Phys. JETP 41, 163 (1975)].
- <sup>22</sup>A. A. Rogachev, Trudy IV Vsesoyuznoi shkoly po fizike poverkhnosti poluprovodnikov (Proc. Fourth All-Union School on Physics of Semiconductor Surfaces), Izd. TGU, 1979, p. 67.
- <sup>23</sup>L. Pauling and P. Pauling, Chemistry, W. H. Freeman, San Francisco, 1975 (Mir, M., 1979, p. 156).
- <sup>24</sup>V. V. Vladimirov, A. F. Volkov, and E. Z. Meĭdikhov, Plazma poluprovodnikov (Semiconductor Plasma), Atomizdat, M., 1978.
- <sup>25</sup>V. S. Bagaev, N. V. Zamkovets, L. V. Keldysh, N. N. Sibel'din, and V. A. Tsvetkov, Zh. Eksp. Teor. Fiz. 70, 1501 (1976) [Sov. Phys. JETP 43, 783 (1976)].
- <sup>26</sup>K. S. Singwi and M. P. Tosi, Phys. Rev. B 23, 1640 (1981).
- <sup>27</sup>V. S. Bagaev, L. V. Keldysh, N. N. Sibel'din, and V. A. Tsvetkov, Zh. Eksp. Teor. Fiz. 70, 702 (1976) [Sov. Phys. JETP 43, 362 (1976)].
- <sup>28</sup>É. I. Rashba, Fiz. Tekh. Poluprovodn. 8, 1241 (1974) [Sov. Phys. Semicond. 8, 807 (1975)].
- <sup>29</sup>E. A. Andryushin, L. V. Keldysh, and A. P. Silin, Zh. Eksp. Teor. Fiz. 73, 1163 (1977) [Sov. Phys. JETP 46, 616 (1977)]; E. A. Andryushin and A. P. Silin, Fiz. Tverd. Tela (Leningrad) 18, 2130 (1976) [Sov. Phys. Solid State 18, 1243 (1976)].
- <sup>30</sup>V. G. Litovchenko, Surf. Sci. 73, 446 (1978).
- <sup>31</sup>V. E. Bisti and A. P. Silin, Fiz. Tverd. Tela (Leningrad) 20, 1850 (1978) [Sov. Phys. Solid State 20, 1068 (1978)].
- <sup>32</sup>V. G. Litovchenko, Osnovy fiziki poluprovodnikovykh sloistykh sistem (Fundamentals of the Physics of Semiconductor Layer Systems), Naukova Dumka, Kiev, 1980.
- <sup>33</sup>G. O. Muller and R. Zimmermann, Proc. Fourteenth Intern. Conf. on Physics of Semiconductors, Edinburgh, 1978, publ. by Institute of Physics, London (1979), p. 165.
- <sup>34</sup>A. A. Rogachev, Prog. Quantum Electron. 6, 141 (1980).
- <sup>35</sup>O. Hildebrand, B. O. Faltermeier, and M. H. Pilkuhn, Solid State Commun. 19, 841 (1976).
- <sup>36</sup>M. S. Brodin, I. V. Blonskiĭ, and V. V. Tishchenko, Pis'ma Zh. Eksp. Teor. Fiz. 32, 119 (1980) [JETP Lett. 32, 108 (1980)].

Translated by A. Tybulewicz